Controlling columnar order in a discotic liquid-crystal by kinetic arrest of disc tumbling

Zhenxuan Chen[1], Camille Bishop[2], Erik Thoms[3], Harald Bock[4], M. D. Ediger[2], Ranko Richert[3], Lian Yu[1,2]*

[1]School of Pharmacy, University of Wisconsin-Madison, Madison, Wisconsin 53705, USA
[2]Department of Chemistry, University of Wisconsin-Madison, Madison, Wisconsin 53705, USA
[3]School of Molecular Sciences, Arizona State University, Tempe, Arizona 85287, USA
[4]Centre de Recherche Paul Pascal, CNRS & Université de Bordeaux, 33600 Pessac, France

* Corresponding author: Lian YU, Email: lian.yu@wisc.edu

Abstract
By cooling at different rates, the discotic liquid crystal (LC) phenanthro[1,2,3,4,ghi]perylene-1,6,7,12,13,16-hexacarboxylic hexaester (PNP) can form glasses of widely different columnar order, including zero order. The temperature at which columnar order is frozen at a given cooling rate corresponds to a slow relaxation mode revealed by dielectric spectroscopy and attributed to disc tumbling within the column. The control of columnar order in this discotic LC is analogous to the control of smectic order in calamitic LCs reported earlier. In both cases, kinetic arrest of a slow molecular rotation above the calorimetric T_g freezes the LC order. This principle can be applied to predict and control molecular packing in the fabrication of organic electronics.

Introduction

A central goal of materials science is to control molecular packing in the solid state as a means to optimize function. Past efforts in this area have largely focused on *crystalline solids*, using crystal polymorphs to access the diversity of structures and properties, while treating amorphous solids and glasses as inherently "structureless" and poor targets for engineering. Recent work has shown that glasses can be prepared to possess different structural order by physical vapor deposition (PVD)[1] and by vitrifying liquid crystal (LC).[2,3] In a PVD process, the preferential molecular alignment at the interface is transferred layer-by-layer to the bulk product, while for glass-forming LCs, it is possible to freeze the different molecular organization in the fluid state into a solid glass. With both approaches, processing conditions can be varied to manipulate structural order in the solid product. The resulting hybrid materials combine the advantages of traditional glasses (spatial uniformity, lack of grain boundaries) with tailored molecular alignment and are potentially useful for applications in organic electronics. [4,5]

Previous work on anisotropic glasses by vitrifying LCs focused on calamitic systems (composed of rod-like molecules) and introduced the notion that kinetic arrest of the slow end-over-end rotation in the fluid state dictates the amount of order in the glass.[2,3] For itraconazole (ITZ) and saperconazole (SAP), cooling an isotropic liquid at different rates produces glasses with different smectic order, including no order, and the resulting order is that reached by the system before the end-over-end rotation is frozen. Because rod-like molecules tend to pack in parallel, the end-over-end rotation is significantly slower (by a factor of 1000 or more) than rotation about the long axis

and undergoes kinetic arrest at a higher temperature.[6,7,8] The fact that LC transitions can be circumvented in this way challenges the common notion that LC transitions are extremely fast,[9,10] and entirely controlled by thermodynamics, as opposed to kinetics.[11,12,13]

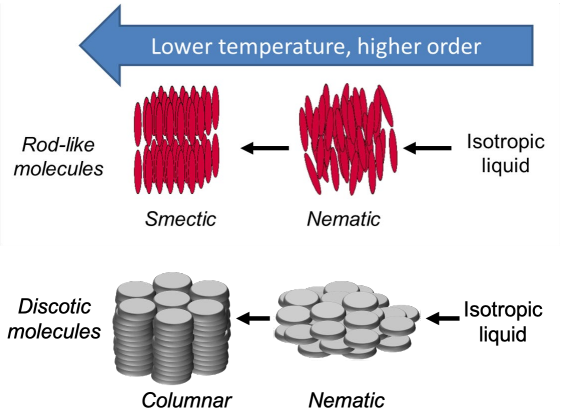

Fig. 1. Analogy between LCs composed of rod-like molecules and discotic molecules. In both cases, cooling an isotropic liquid may lead to orientational ordering (nematic phase) and positional ordering (smectic phase for rods, columnar phase for discs).

In this work, we investigate the kinetic control of LC order in a discotic system. As illustrated in Fig. 1, discotic LCs have analogous phase transitions to calamitic LCs.[14,15] In both cases, cooling the isotropic liquid may lead to orientational ordering (nematic phase) and positional ordering (smectic phase for rods, columnar phase for discs). As in the case of calamitics, discotic systems can have multiple relaxation modes,[16,17] thus multiple glass transition temperatures. Given these similarities, discotic LCs offer an interesting test for our hypothesis of the kinetic control of LC order and the condition for preparing anisotropic glasses.

Like their calamitic counterparts, discotic LCs have important applications in organic electronics.[18,19,20,21] In this context, columnar LC structures produced by discotic molecules are especially promising for enhancing charge mobility along the columns. For example, hole mobility can be enhanced for columnar structures used as field-effect transistors.[19] Charge carrier mobility in a columnar LC diode was increased by 5 orders of magnitude with improved LC order.[20] The system chosen for this study, phenanthro[1,2,3,4,ghi]perylene-1,6,7,12,13,16-hexacarboxylic hexaester (PNP, Scheme 1) has a columnar LC phase ($T_{Col/I}$ = 519 K), which upon cooling vitrifies at 393 K (T_g).[22] The aromatic core of PNP was designed to suppress crystallization and stabilize its columnar LC phase at room temperature, while maintaining its electronic properties.[22] Bishop et al. studied the glasses of PNP prepared by PVD and found that the columnar order in thin films can be systematically tuned by deposition temperature and deposition rate.[23] The system offers a large temperature window between $T_{Col/I}$ and the glass transition temperature to allow the development of columnar order, a useful feature for testing our hypothesis.

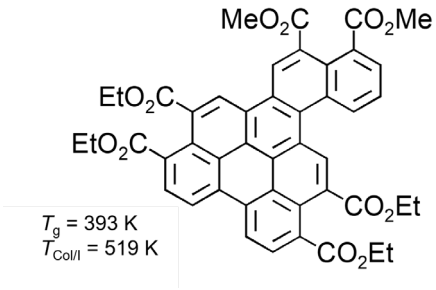

Scheme 1. Molecular structure of PNP and transition temperatures.

We show that columnar order in a bulk PNP glass can be altered and even eliminated by cooling at different rates. Slow cooling (e.g., 1 K/min) leads to glasses with strong columnar order, while the order is diminished by faster cooling and eliminated by cooling faster than 50 K/s. The timescale associated with the freezing of columnar order corresponds to a slow relaxation mode (δ relaxation) identified by dielectric spectroscopy (DS), assigned to the hindered tumbling of the disc in a column. Our result supports the previous conclusion reached for calamitic systems that

LC transitions are kinetically controlled by rate-limiting molecular rotations (end-over-end rotation for rods, heads-over-tails flip for discs) and that manipulating the condition of kinetic arrest allows control of LC order.

Experimental Section

The discotic LC molecule PNP (Scheme 1) was synthesized using the procedure described by Kelber et al.[22]

Differential Scanning Calorimetry (DSC) was performed with a TA 2000 unit. A sample (about 3 mg) in an aluminum pan was heated and cooled at controlled rates to determine the glass transition temperature (T_g) and columnar-to-isotropic-liquid transition temperature ($T_{Col/I}$).

X-ray scattering was performed in transmission geometry on a Bruker D8 Discover diffractometer. A capillary tube (Charles Supper, MA, 0.7 mm OD, 10 μm wall thickness) containing a sample was irradiated perpendicularly by the Cu Kα source beam 2 mm in diameter. Scattered X-ray was detected with a Vantec 500 area detector 19.92 cm from the sample and since our sample was not aligned, the pattern was integrated azimuthally to produce a one-dimensional profile. Temperature was controlled by an Instec mK2000 heating stage. The scattering pattern of the empty capillary was collected as background. Silver behenate was used to calibrate diffraction angles and to determine instrumental resolution.[24] Measured on our instrument, the full width at half maximum (FWHM) of the low-angle silver behenate diffraction peaks was $\sigma = 0.018$ Å^{-1}, while the intrinsic width is $\sigma_0 = 0.006$ Å^{-1}, corresponding to its correlation length of ~100 nm.[24] From these values, we obtained the instrument resolution: $\sigma_{inst} = (0.018^2 - 0.006^2)^{1/2} = 0.017$ Å^{-1}. Crystalline powder of PNP was packed in a capillary tube and flame sealed. The sample was heated above $T_{Col/I}$ and cooled at a controlled rate to form glasses. Cooling rates slower than 0.17 K/s were achieved with the DSC sample cell; the rate 20 K/s was achieved by air-cooling the sample from 573 K to room temperature; the rate 50 K/s was achieved by plunging a 573 K sample into an ice/water bath. The cooling rates of 20 and 50 K/s were determined by performing the same cooling procedures with a thermocouple coated by a thin layer of epoxy to simulate the thermal conductivity of the capillary wall. The cooling rate was measured near $T_{Col/I}$.

For dielectric spectroscopy, PNP powder was mixed with a small amount of silica beads (∅ = 9.2 μm) as spacers. This mixture was placed on a brass electrode (∅= 20 mm) and melted by heating above $T_{Col/I}$ (typically 540 K) under dry nitrogen for ten minutes. A smaller (∅ = 8.1 mm), preheated brass electrode was placed over the melt, and the complete capacitor was cooled by contact with a refrigerated metal slab before measurement. The diameter of the silica beads did not provide a good estimate for the electrode separation, which is required to obtain correct values for permittivity. Therefore, the actual separation was determined from the height difference of the filled and empty capacitor at ambient temperature.

Dielectric measurements were performed with a Solartron Instruments SI-1260 Impedance/Gain-Phase Analyzer (1 Hz ≤ ν ≤ 1 MHz) combined with a DM-1360 interface, employing a Novocontrol Quatro cryosystem for temperature control ($T \leq 430$ K; $\Delta T = 0.1$ K). A second setup, facilitating measurements at higher temperatures and shorter times for each spectrum, made use of

a home-built resistive heater regulated by a Lakeshore Model 330 temperature controller ($T \leq 550$ K; $\Delta T = 1$ K). The measurements were performed by a HP-4284A precision LCR meter (100 Hz $\leq \nu \leq$ 1 MHz). The sample was held in a dry nitrogen stream during all dielectric measurements.

Results and Discussion

Fig. 2 shows the DSC result of a PNP liquid during cooling (blue trace) and subsequent heating (red trace). During cooling, the isotropic liquid transforms to a columnar phase at $T_{Col/I}$ = 519 K (onset) with an enthalpy change of 8.2 J/g, which undergoes a glass transition at T_g = 393 K (onset). Upon reheating, the glass transforms to a liquid at T_g, and the liquid crystallizes near 450 K. The crystals melt near 490 K at two distinct temperatures (T_{m1} and T_{m2}), indicating polymorphism. The resulting liquid is the columnar LC, which transforms to the isotropic liquid at $T_{Col/I}$.

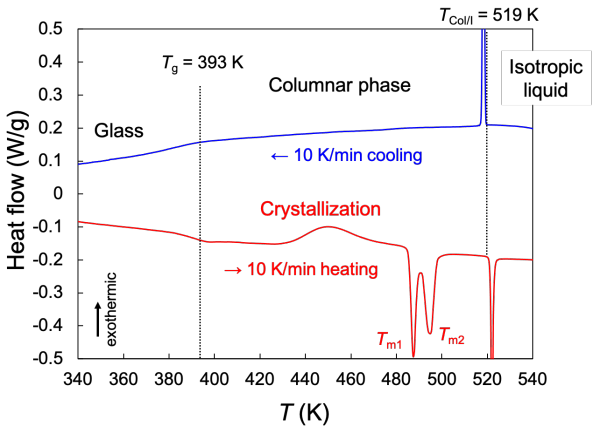

Fig. 2. DSC traces of PNP during cooling and the subsequent reheating.

We use X-ray scattering to characterize several aspects of the columnar structure in PNP, including inter-column spacing, correlation length, and amplitude of density modulation. Fig. 3a shows the scattering patterns of a PNP liquid as it is cooled from the isotropic liquid. Below $T_{Col/I}$, strong scattering was detected (see inset of Fig. 3a for a representative scattering pattern), indicative of columnar order. The primary feature is a uniform ring at q_1 = 0.41 Å^{-1}, corresponding to columns separated by 15 Å ($2\pi/q_1$), approximately the diameter of the molecule. The uniform ring in the scattering pattern indicates absence of preferred alignment in our sample (a Debye powder). In addition to the q_1 peak, weaker peaks are seen at 0.71 and 0.82 Å^{-1}, corresponding to higher-order diffractions of hexagonally packed columns at $\sqrt{3}\,q_1$ and $2q_1$, respectively.[22, 23] The weak higher-order

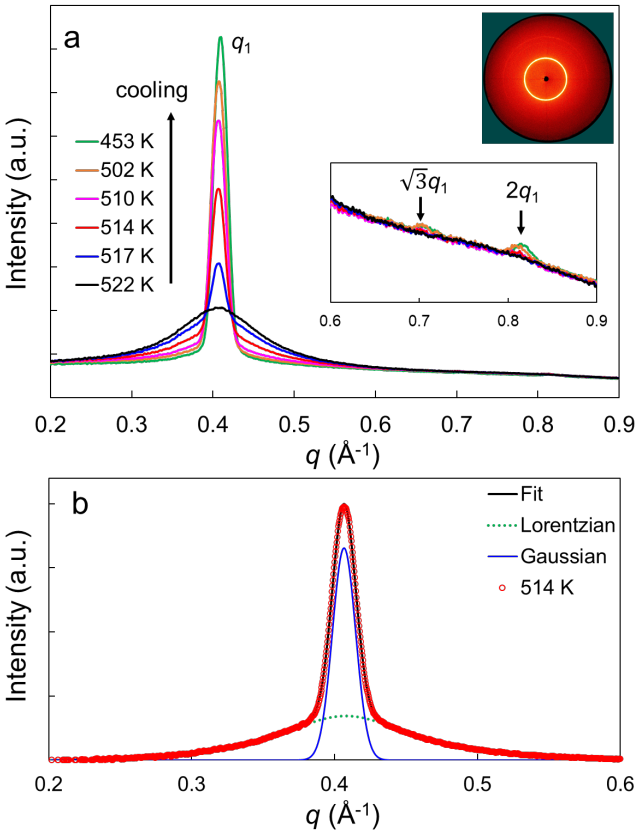

Fig. 3. (a) X-ray scattering patterns of PNP during cooling. The insets are the 2D scattering pattern and enlarged view of the region 0.6 – 0.9 Å^{-1} showing higher-order diffraction peaks. (b) Decomposition of the primary diffraction peak at 514 K into a broad Lorentzian and a sharp Gaussian.

diffractions indicate a nearly sinusoidal inter-column density modulation. In addition to columnar order, Kelber et al. have observed π stacking order in this system, giving rise to a scattering peak at 1.8 $Å^{-1}$ and corresponding to a real-space distance of 3.5 Å.[22] In this work, we only focus on the columnar order.

We find that each diffraction peak can be fitted as a sum of a sharp Gaussian component and a broad Lorentzian component, see Fig. 3b. The FWHM for the broad Lorentzian component is approximately 0.12 $Å^{-1}$, well exceeding the instrument resolution (σ_{inst} = 0.017 $Å^{-1}$, see Experimental Section). This broad component is present even above $T_{Col/I}$, i.e., in the isotropic phase, and decreases as the sharp component grows with cooling below $T_{Col/I}$ (see Fig. 4 below). The broad component arises from the excluded volume effect – the ordering effect of each molecule on its neighbors.[25] Because the internal volume of each molecule is not penetrated by its neighbors, molecules pack in a liquid in a way that conforms to the shape of the molecule, in our case a disc 15 Å in diameter, thus creating a positional order. Judging from the width of the broad Lorentzian, this positional order has a correlation length of 50 Å (3 columns). Similar excluded-volume peaks have been observed in other LC systems such as ITZ and SAP.[2,3] In contrast to the broad component, the Gaussian peak is much sharper, with a FWHM of 0.019 $Å^{-1}$, just barely above the instrument resolution (0.017 $Å^{-1}$). From these values, we estimate the intrinsic peak width for the columnar order in PNP to be 0.008 $Å^{-1}$, corresponding to a correlation length of 70 nm.

Fig. 4 shows how columnar order evolves with cooling below $T_{Col/I}$. Fig. 4a shows the scattering strength (derived from the area of the peaks), indicative of the amplitude of density modulation; Fig. 4b shows the q_1 value, indicative of inter-column spacing. From Fig. 4a, we see that upon cooling below $T_{Col/I}$, the area of the sharp Gaussian component of the scattering peak, A_G, rises sharply, while the area of the broad Lorentzian component, A_L, decreases. This confirms that the sharp Gaussian peak is associated with columnar order, while the broad Lorentzian peak with the excluded volume effect. In what follows, we use A_G as a measure of columnar order. With cooling below $T_{Col/I}$, columnar order reaches a maximum near 450 K and decreases at lower temperatures. The rate of decrease appears to slow down below the calorimetric T_g (393 K). The rise and fall of PNP's columnar order in this manner is noteworthy since many LCs show steady increase of order with cooling below the clearing temperature.[26] The PNP behavior could be a

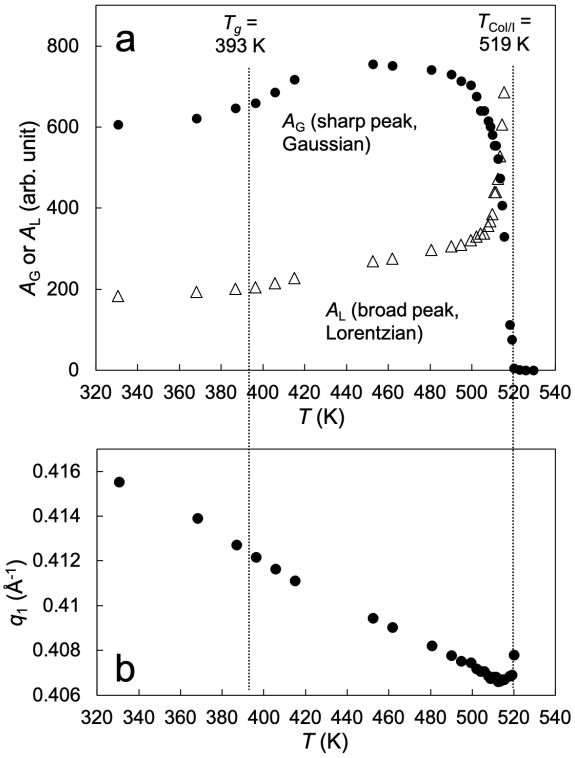

Fig. 4. Temperature dependence of columnar order with cooling from the isotropic liquid state at a rate of 0.017 K/s. (a) The areas of the sharp Gaussian component, A_G, and the broad Lorentzian component, A_L. (b) Peak position q_1 indicative of inter-column spacing. The range 440 – 420 K was skipped to avoid crystallization.

result of stress that develops from the mismatch of thermal expansion coefficients of the LC and the container, which is slow to relax in its viscous state approaching T_g. [27,28]

In Fig. 4b, we plot the peak position q_1 as a function of temperature. Notice the nearly linear increase of q_1 with falling temperature, insensitive to the passage of T_g. This trend indicates that with cooling, the inter-column spacing ($2\pi/q_1$) decreases; the corresponding thermal expansion coefficient is 117 ppm/K, typical of molecular solids. The almost linear dependence of q_1 on temperature is in contrast with the complicated evolution of scattering strength A_G during cooling. This indicates that the two aspects of the columnar structure – amplitude of density modulation and inter-column spacing – are not tightly correlated. The inter-column spacing is largely controlled by thermal expansion, while the "perfection" of columnar order is far more sensitive to the degree of cooling below $T_{Col/I}$.

We find that the cooling rate has a significant influence on the columnar order in the PNP glass. Fig. 5 illustrates this effect with glasses prepared at three different cooling rates: R_c = 0.017, 20, and 50 K/s. All these glasses were analyzed at a common temperature, 368 K, i.e., 25 K below T_g. The glass prepared at the slowest cooling rate had the highest columnar order, and the order decreased as cooling rate increased. At R_c = 50 K/s, columnar order was absent and only a broad Lorentzian scattering peak was observed, which arose from the excluded volume effect. Furthermore, the disappearance of columnar order by fast cooling is accompanied by the elimination of the π stacking peak at 1.8

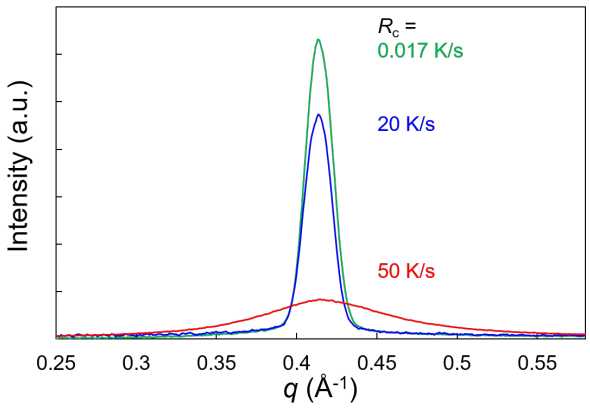

Fig. 5. X-ray scattering patterns of PNP glasses prepared by cooling at different rates indicated. These glasses are compared at 368 K (T_g – 25 K).

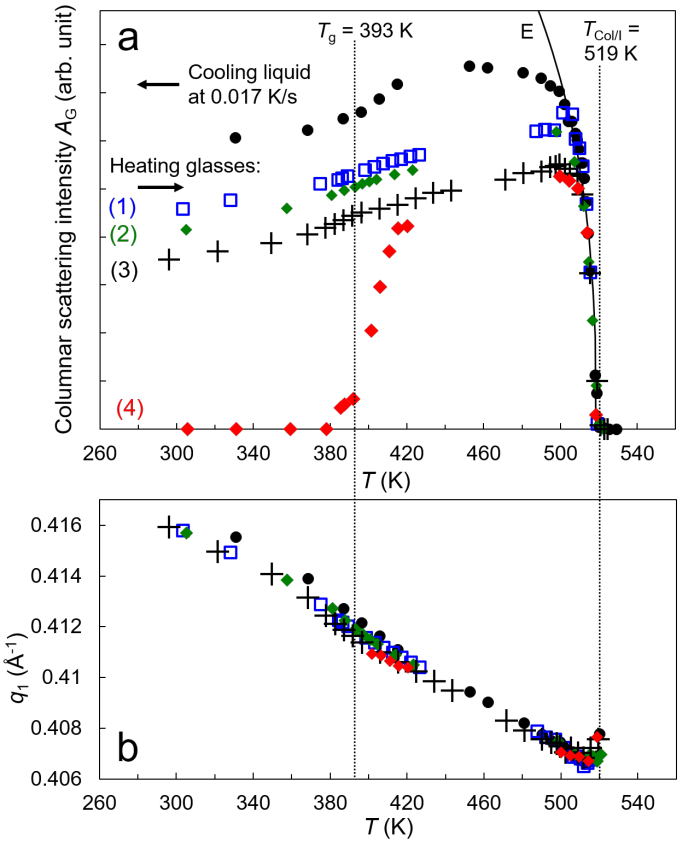

Fig. 6. Evolution of columnar order in 5 samples of PNP. (a) Scattering strength A_G. The top trace is for cooling an isotropic liquid at 0.017 K/s (A_G trace in Fig. 4a); the others correspond to heating Glasses 1 to 4 prepared at different cooling rates R_c: (1) 0.05 K/s, (2) 0.17 K/s, (3) 20 K/s, and (4) 50 K/s. The cooling and heating curves join above 500 K reaching the equilibrium columnar order (Curve E). (b) q_1 for the same samples.

$Å^{-1}$ (see Figure S1), indicating the two structural features are associated with each other.

To establish the condition of kinetic arrest leading to the order observed, we show in Fig. 6 the evolution of columnar order as the glasses of PNP are heated. For reference, the results in Fig. 4 are included here to show the behavior during cooling from the isotropic phase. The four glasses in Fig. 6 (1 – 4) were prepared at different cooling rates and possessed different columnar order before heating. The data shown in Fig. 6 were recorded as these glasses were heated. Of them, Glass 4 had no columnar order as-prepared due to very fast cooling (50 K/s). As shown in Fig. 6a, during heating, columnar order in Glass 4 remained absent until T_g was reached; above T_g, the order rose quickly, eventually merging near 510 K with the top trace (measured by cooling down from the isotropic liquid). For Glasses 1, 2, and 3, slower cooling rates were used for preparation and columnar order was present before heating. For these samples, columnar order increased slightly during heating up to ~500 K, with no abrupt jump as seen in Glass 4. Near 500 K, all heating curves merged with the cooling curve.

We interpret these results as follows. Cooling at different rates produces glasses of different columnar order, all below the equilibrium order. With heating, the system endeavors to reach equilibrium, but succeeds only when heated to high enough temperatures. In Fig. 6a, the region above 500 K represents the equilibrium behavior where cooling and heating curves merge and where the same columnar order is reached from two opposite directions - cooling and heating. The curve labeled E in Fig. 6a is a power-law fit of this equilibrium region.[26] Below 500 K, the system is stranded in different out-of-equilibrium states. For Glasses 1, 2, and 3, columnar order changes modestly with temperature, in a quasi-linear manner, and we attribute this to the small perturbation of the frozen-in columnar order by thermal expansion and stress relaxation. Following this reasoning, a "fictive temperature" can be assigned for the columnar order in each glass, namely, the temperature at which kinetic arrest occurs when cooling the precursor liquid to yield the columnar order observed in the glass. For Glasses 1, 2, and 3, this temperature, T_{arrest}, is the temperature at which frozen-in columnar order merges with the equilibrium curve (Curve E) during heating. Table 1 shows the T_{arrest} values thus obtained. For Glass 4 (prepared at the fastest cooling rate), no columnar order was present at low temperatures, but it gained order when heated above T_g, possibly a result of the low-stability structure produced by fast cooling. For this glass, any molecular motion that leads to columnar ordering must have been frozen above $T_{Col/I}$, so no order could develop. Later, we will use the results in Table 1 to infer a relaxation mode responsible for the development of columnar order.

Table 1. Temperature at which columnar order is frozen as a function of cooling rate R_c.[a]

R_c (K/s)	T_{arrest} (K)
0.017	502
0.05	505
0.17	507
20	510
50	519

[a] The error in T_{arrest} is approximately 1 K.

In Fig. 6b, we compare the inter-column spacing for PNP glasses prepared at different cooling rates. By and large, the cooling rate has only a small effect on this aspect of columnar structure: despite their different columnar order (scattering strength shown in Fig. 6a), the different glasses feature virtually the same inter-column spacing. Only on close inspection do we detect a small increase of inter-column spacing for glasses prepared at faster cooling rates. This effect is barely discernable in Fig. 5 by comparing the positions of the two larger peaks (the smallest peak has no sharp columnar scattering and only broad scattering due to the excluded volume effect).

To investigate the kinetic control of columnar order, we determined the timescales of molecular motions by DS and DSC. Fig. 7 shows representative dielectric spectra at three temperatures. At 353 K (Fig. 7a), a broad peak is seen in the loss spectrum ε'', accompanied by a step-like change in permittivity ε'. This peak is a superposition of two strongly broadened relaxations, termed γ_1 and γ_2. With heating, both peaks shift to higher frequencies, as shown in Fig. 8. At 480 K (Fig. 7b), the high-frequency end of the loss spectrum ε'' (100 kHz – 1 MHz) is the low-frequency flank of the double peak described above, while the low-frequency end is the dc-conductivity with a characteristic frequency dependence $\varepsilon'' \sim \nu^{-1}$. These two features, however, do not fully account for the intermediate range of the 480 K spectrum, namely, the minimum at 10 kHz in loss and the accompanying step in permittivity. An additional relaxation process, termed α, is required to account for the observed spectra. The α process is also depicted in Fig. 8, and it is associated with the calorimetric glass transition (see below). Finally, at 527 K (Fig. 7c), electrode polarization (EP) causes an apparent increase in ε' at low frequencies (< 10 kHz), but close examination reveals a shoulder that corresponds to an additional low frequency relaxation, termed δ. The loss spectrum is less informative about the δ process, being dominated by dc conductivity.

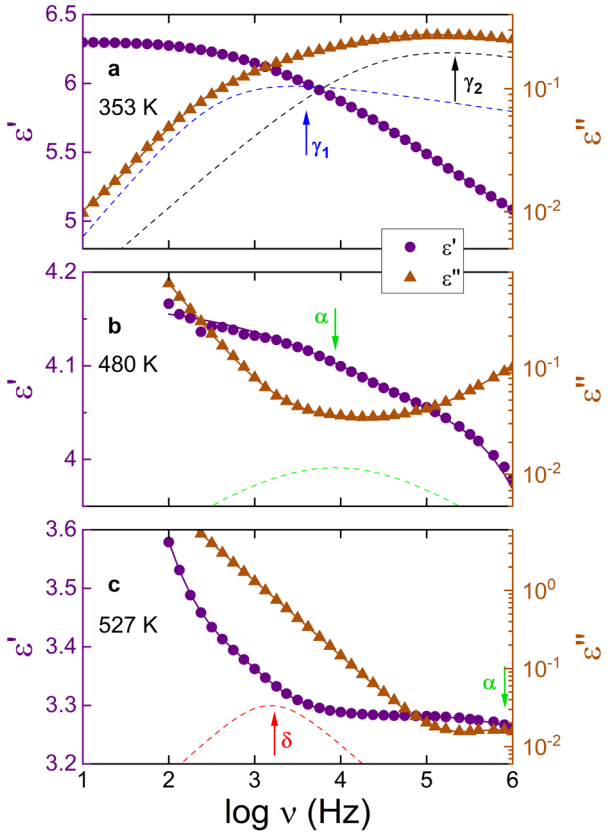

Fig. 7. Exemplary dielectric spectra at 353 K (a), 480 K (b), and 527 K (c), shown as permittivity ε' (left axis, purple circles) and loss ε'' (right axis, brown triangles). The continuous lines are fits of the spectra to Eq. 1. The thin dashed lines and arrows of the same colors indicate the relaxation modes (δ, α, γ_1, and γ_2) in the loss spectra.

The quantitative relaxation times plotted in Fig. 8 are obtained by fitting the dielectric spectra. Each spectrum is modeled as the sum of the relevant contributions, including the observed relaxation modes as well as EP (each represented by a Havriliak-Negami term) and the dc conductivity. The full model is given by:[29]

$$\varepsilon^*(\omega) = \varepsilon_\infty + \sum_j \frac{\Delta\varepsilon_j}{\left(1+(i\omega\tau_j)^{1-\alpha_j}\right)^{\beta_j}} + \frac{\sigma_{dc}}{i\omega\varepsilon_0}, \qquad (1)$$

where j is up to 3 (up to three relaxations included at the same time). Here, $\omega = 2\pi\nu$ is the angular frequency, ε_∞ the permittivity at very high frequencies, and ε_0 the vacuum permittivity. $\Delta\varepsilon_j$ and τ_j denote the dielectric relaxation amplitude and relaxation time constant, while α and β are the symmetrical and asymmetrical broadening parameters. All fits were performed simultaneously on the real (ε') and imaginary (ε'') parts of $\varepsilon^* = \varepsilon' - i\varepsilon''$.

In addition to dielectric spectroscopy, DSC was used to measure the mobility associated with the calorimetric glass transition. The onset of DSC T_g (Fig. 2) was measured as a function of cooling rate R_c, and the results are shown in Fig. 8 along with the results of DS. The lower points in Fig. 8 are the most probable relaxation times for the four relaxation modes determined by DS, shown as functions of temperature. The DSC T_g is displayed using the same temperature axis as a function of R_c indicated on the right y axis. This way of plotting the DSC and DS results together is based on the condition of kinetic arrest:

$$\tau\,(T_g)\,R_c = C \qquad (2)$$

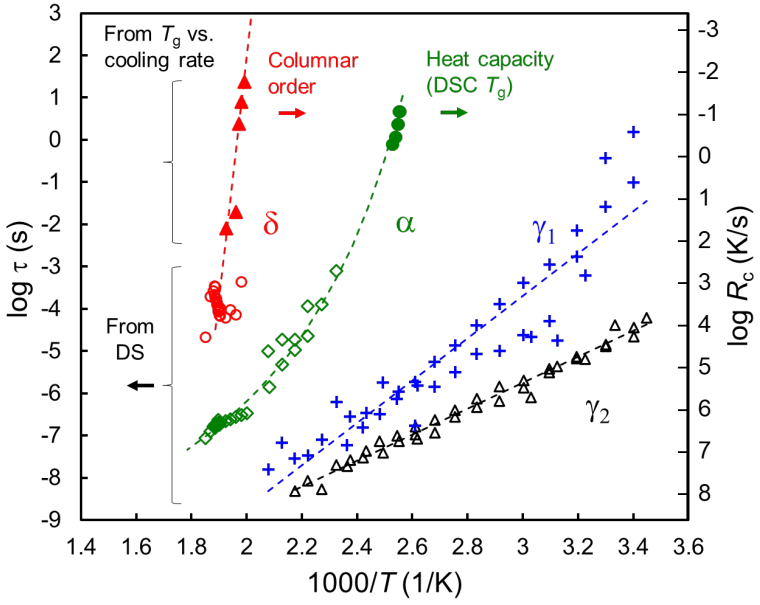

Fig. 8 Relaxation map of PNP. Relaxation times from DS (open symbols and +) are plotted using the left y axis. T_g vs. cooling rate results (solid symbols) are plotted using the right y axis where the properties undergoing kinetic arrest are heat capacity (DSC T_g) and columnar order. The two y axes are related by $\tau\,(T_g)\,R_c = C$ with $C = 0.4$ K. The error in DSC T_g is approximately 0.1 K. The error in relaxation times is 0.1 decade on average.

where $\tau\,(T_g)$ is the relaxation time at T_g and C is a constant. The value of C depends on the way T_g is defined (the onset, the midpoint, or the endpoint of the glass transition; measured during heating or cooling).[30,31] For our definition of T_g (onset during cooling), $C = 0.4$ K holds for molecular glasses,[2,3,32,33] and this value is used to construct Fig. 8. Of the four relaxation modes detected by DS, the α process is associated with the DSC T_g. The faster γ_1 and γ_2 processes are assigned to side-chain fluctuations, in analogy with the assignment for other discotic LCs.[16,17] The high dielectric strength of PNP's γ_1 and γ_2 processes (Fig. 7) is consistent with its polar side chains and non-polar core (Scheme 1), for which side-chain fluctuations are expected to strongly modulate the dipole moment. In addition, we assign the slow δ process to the tumbling of discs in a columnar LC, and the faster α process to the rotation of the disc about the column axis. This assignment is in analogy with the relaxation modes for calamitic LCs[3,6] and consistent with the literature on discotic LCs. For a hexa-*peri*-hexabenzocoronene, the DSC T_g was associated with the dielectric α process and with the axial disc rotation, while a slower

dielectric process is assigned to the out-of-plane tumbling of the disc.[17] For other systems, dielectric relaxation modes were interpreted in a similar manner.[34,35]

Analogous to the calorimetric T_g as a function of cooling, we have included in Fig. 8 the temperature of kinetic arrest for the columnar order at each cooling rate (Table 1). These data points are located at high temperatures, near the δ mode, and mark the location of a hypothetical relaxation mode that controls the freezing of columnar order. It is evident that this mode is not associated with the α process, the γ_1 process, or the γ_2 process, since the corresponding T_g at our cooling rates far exceeds any observed arrest temperature. The δ mode, on the other hand, is a possible candidate since it matches very well the proposed relaxation responsible for columnar ordering. For this reason, we group together the data points from the two measurements as defining the δ process in PNP and conclude that this process controls its columnar ordering.

In the procedure above, we use the temperature at which columnar order is frozen at a given cooling rate to propose a previously unknown relaxation mode (δ). This procedure is conceptually similar to the use of calorimetric T_g to deduce a relaxation process. In the latter method, a liquid's heat capacity is monitored during cooling (or heating) and the decrease (increase) of heat capacity marks the kinetic arrest of relevant degrees of freedom. Variation of cooling (heating) rate then enables determination of the temperature dependence of the mobility associated with the calorimetric T_g.

Given that it is a new procedure to use the freezing of LC order to deduce a relaxation mode, we illustrate the method in Fig. 9 with further examples using the published results on two calamitic systems: ITZ and SAP.[2,3] Fig. 9 shows the two relaxation times, τ_α and τ_δ, determined by DS for each system.[3,6] The α process is associated with the fast rotation of the rod-like molecules about the long axis and the δ process with the slow end-over-end rotation. For these systems, cooling at different rates prepares glasses with different smectic order, including no order. From the order trapped in the glass and the equilibrium order as a function of temperature (the counterpart of Fig. 6a), we determine the temperature at which smectic order is frozen at a given cooling rate.

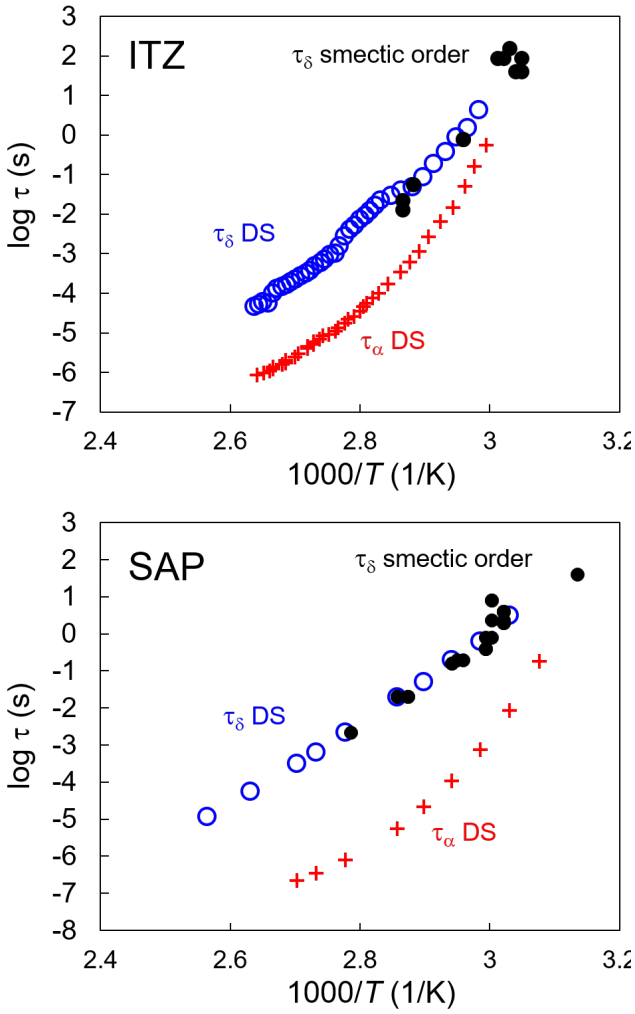

Fig. 9. Relaxation maps of ITZ and SAP. τ_α DS and τ_δ DS are relaxation times determined by dielectric spectroscopy.[3,6] τ_δ smectic order (black circles) indicates the relaxation times inferred by the kinetic arrest of smectic order.

We then convert the cooling rate to a relaxation time using Eq. 2. This yields pairs of time-temperature points that are plotted in Fig. 9 as black circles. These points depict the hypothetical relaxation mode responsible for the kinetic arrest of smectic order. Fig. 9 shows that the proposed relaxation mode closely matches the δ process observed by DS, but not the α process. This indicates that the freezing of smectic order in these systems is associated with the kinetic arrest of the end-over-end rotation. While this conclusion was reached by previous work,[2,3] our purpose here is to draw attention to a new method to identify relaxation modes that might be hidden from calorimetric and dielectric probes.

Conclusions

In this work a discotic LC is used to test the principle of the kinetic control of LC order established earlier with calamitic systems.[2,3] By cooling at different rates, the discotic LC PNP can form glasses that have widely different columnar order, including zero order. The temperature at which columnar order freezes at a given cooling rate reveals a relaxation mode that is confirmed by dielectric spectroscopy and associated with the slow tumbling of discs in a column. The control of columnar order in this way is analogous to the control of smectic order of LCs composed of rod-like molecules reported earlier. In both cases, kinetic arrest of a slow molecular rotation (end-over-end rotation for rods, heads-over-tails flip for discs) above the calorimetric T_g controls the LC order frozen into the glass. This work thus generalizes the previous finding to a new class of LCs. Relative to the previously studied calamitic systems, the PNP system is characterized by slower equilibration of its columnar order, even well above the calorimetric T_g (Fig. 6a), broadening the diversity of test cases. Our finding can be used to predict and control molecular packing in the fabrication of organic electronics. We anticipate the principle to be applicable to other methods of glass formation beyond liquid cooling, such as vapor deposition and solvent evaporation. These other modes of glass formation present different environments than in a bulk fluid in which kinetic arrest occurs for the rate-limiting motion that controls LC ordering. It is of interest to investigate the effect of cooling rate on other aspects of the columnar structure, including the π stacking order.

Acknowledgements

We thank the NSF (DMR-1904601) for supporting this work and acknowledge the use of NSF-supported facilities through the University of Wisconsin Materials Research Science and Engineering Center (DMR-1720415).

References

[1] Ediger, M.; de Pablo, J.; Yu, L. Anisotropic Vapor-Deposited Glasses: Hybrid Organic Solids. *Acc. Chem. Res.* **2019**, *52* (2), 407-414.

[2] Teerakapibal, R.; Huang, C.; Gujral, A.; Ediger, M. D.; Yu, L. Organic glasses with tunable liquid-crystalline order. *Phys. Rev. Lett.* **2018,** *120* (5), 055502.

[3] Chen, Z.; Yu, J.; Teerakapibal, R.; Meerpoel, L.; Richert, R.; Yu, L. Organic Glasses with Tunable Liquid-Crystalline Order Through Kinetic Arrest of End-Over-End Rotation: The Case of Saperconazole. *Soft Matter* **2020**, *16* (8), 2025-2030

[4] Chen, H.-M. P.; Ou, J. J.; Chen, S. H. Glassy liquid crystals as self-organized films for robust optoelectronic devices. In *Nanoscience with Liquid Crystals*; Li , Q., Ed.; Springer: 2014; pp 179-208.
[5] Iino, H.; Usui, T.; Hanna, J.-i. Liquid crystals for organic thin-film transistors. *Nat. Commun.* **2015,** *6*, 6828.
[6] Tarnacka, M.; Adrjanowicz, K.; Kaminska, E.; Kaminski, K.; Grzybowska, K.; Kolodziejczyk, K.; Wlodarczyk, P.; Hawelek, L.; Garbacz, G.; Kocot, A.; Paluch, M. Molecular dynamics of itraconazole at ambient and high pressure. *Phys. Chem. Chem. Phys.* **2013,** *15* (47), 20742-20752.
[7] Schonhals, A.; Kremer, F. *Broadband Dielectric Spectroscopy*. Springer: Berlin, 2003; pp 385-432.
[8] Brás, A.; Dionísio, M.; Huth, H.; Schick, C.; Schönhals, A. Origin of glassy dynamics in a liquid crystal studied by broadband dielectric and specific heat spectroscopy. *Phys. Rev. E* **2007,** *75* (6), 061708.
[9] Wouters, S.; Demir, F.; Beenaerts, L.; Van Assche, G. Calibration and performance of a fast-scanning DSC—Project RHC. *Thermochim. Acta* **2012,** *530*, 64-72.
[10] Jiang, J.; Zhuravlev, E.; Huang, Z.; Wei, L.; Xu, Q.; Shan, M.; Xue, G.; Zhou, D.; Schick, C.; Jiang, W. A transient polymorph transition of 4-cyano-4′-octyloxybiphenyl (8OCB) revealed by ultrafast differential scanning calorimetry (UFDSC). *Soft Matter* **2013,** *9* (5), 1488-1491.
[11] Maier, W.; Saupe, A. Eine einfache molekulare Theorie des nematischen kristallinflüssigen Zustandes. *Z. Naturforsch. A* **1958,** *13* (7), 564-566.
[12] McMillan, W. L. Simple molecular model for the smectic A phase of liquid crystals. *Phys. Rev. A* **1971,** *4* (3), 1238.
[13] de Gennes, P. G. An analogy between superconductors and smectics A. *Solid State Commun.* **1972,** *10* (9), 753-756.
[14] Bushby, R.; Lozman, O. Discotic Liquid Crystals 25 Years on. *Curr. Opin. Colloid Interface Sci.* **2002**, *7* (5-6), 343-354.
[15] Sergeyev, S.; Pisula, W.; Geerts, Y. H. Discotic liquid crystals: A new generation of organic semiconductors. *Chem. Soc. Rev*. **2007**, 36, 1902−1929.
[16] Groothues, H.; Kremer, F.; Collard, D.; Lillya, C. Dynamic Properties of Discotic Liquid Crystals with Triphenylene And Benzene Cores, Studied by Broadband Dielectric Spectroscopy. *Liq. Cryst.* **1995**, *18* (1), 117-121.
[17] Elmahdy, M.; Floudas, G.; Mondeshki, M.; Spiess, H.; Dou, X.; Müllen, K. Origin of The Complex Molecular Dynamics in Functionalized Discotic Liquid Crystals. *Phys. Rev. Lett.* **2008**, *100* (10), 107801.
[18] Pisula, W.; Zorn, M.; Chang, J. Y.; Müllen, K.; Zentel, R. Liquid crystalline ordering and charge transport in semiconducting materials. *Macromol. Rapid Commun.* **2009,** *30* (14), 1179-1202.
[19] O'Neill, M.; Kelly, S. M. Ordered materials for organic electronics and photonics. *Adv. Mater.* **2011,** *23* (5), 566-584.
[20] Eccher, J.; Faria, G. C.; Bock, H.; von Seggern, H.; Bechtold, I. H. Order induced charge carrier mobility enhancement in columnar liquid crystal diodes, *ACS Appl. Mater. Interfaces* **2013**, *5*, 11935−11943.
[21] Feng, X. L.; Marcon, V.; Pisula, W.; Hansen, M. R.; Kirkpatrick, J.; Grozema, F.; Andrienko, D.; Kremer, K.; Müllen, K. Towards high charge-carrier mobilities by rational design of the shape and periphery of discotics. *Nat. Mater.* **2009**, *8*, 421-426.

[22] Kelber, J.; Achard, M.-F.; Durola, F.; Bock, H. Distorted Arene Core Allows Room-Temperature Columnar Liquid-Crystal Glass with Minimal Side Chains. *Angew. Chem., Int. Ed.* **2012,** *51*, 5200−5203.
[23] Bishop, C.; Chen, Z.; Toney, M.; Bock, H.; Yu, L.; Ediger, M. Using Deposition Rate And Substrate Temperature To Manipulate Liquid Crystal-Like Order In A Vapor-Deposited Hexagonal Columnar Glass. *J. Phys. Chem. B* **2021**, *125* (10), 2761-2770.
[24] Huang, T.; Toraya, H.; Blanton, T.; Wu, Y. X-Ray Powder Diffraction Analysis of Silver Behenate, A Possible Low-Angle Diffraction Standard. *J. Appl. Cryst.* **1993**, *26* (2), 180-184.
[25] McMillan, W. X-Ray Scattering from Liquid Crystals. I. Cholesteryl Nonanoate and Myristate. *Phys. Rev. A* **1972**, *6* (3), 936-947.
[26] Kapernaum, N.; Giesselmann, F. Simple Experimental Assessment of Smectic Translational Order Parameters. *Phys. Rev. E* **2008**, *78* (6), 062701.
[27] Manjuladevi, V.; Pratibha, R.; Madhusudana, N. Phase Transitions in Liquid Crystals Under Negative Pressures. *Phys. Rev. Lett.* **2002**, *88* (5), 055701.
[28] Powell, C.; Chen, Y.; Yu, L. Fracture of Molecular Glasses Under Tension and Increasing Their Fracture Resistance with Polymer Additives. *J. Non-Cryst. Solids* **2015**, *429*, 122-128.
[29] Havriliak, S.; Negami, S. A complex plane representation of dielectric and mechanical relaxation processes in some polymers. *Polymer* **1967,** *8*, 161-210.
[30] Hensel, A.; Schick, C. Relation between freezing-in due to linear cooling and the dynamic glass transition temperature by temperature-modulated DSC. *J. Non-Cryst. Solids* **1998,** *235*, 510-516.
[31] Dhotel, A.; Rijal, B.; Delbreilh, L.; Dargent, E.; Saiter, A. Combining Flash DSC, DSC and broadband dielectric spectroscopy to determine fragility. *J. Therm. Anal. Calorim.* **2015,** *121* (1), 453-461.
[32] Moura Ramos, J.; Taveira-Marques, R.; Diogo, H. Estimation of The Fragility Index Of Indomethacin By DSC Using The Heating And Cooling Rate Dependency Of The Glass Transition. *J. Pharm. Sci.* **2004**, *93* (6), 1503-1507.
[33] Wojnarowska, Z.; Adrjanowicz, K.; Wlodarczyk, P.; Kaminska, E.; Kaminski, K.; Grzybowska, K.; Wrzalik, R.; Paluch, M.; Ngai, K. Broadband Dielectric Relaxation Study at Ambient and Elevated Pressure of Molecular Dynamics of Pharmaceutical: Indomethacin. *J. Phys. Chem. B* **2009**, *113* (37), 12536-12545.
[34] Yildirim, A.; Bühlmeyer, A.; Hayashi, S.; Haenle, J.; Sentker, K.; Krause, C.; Huber, P.; Laschat, S.; Schönhals, A. Multiple Glassy Dynamics in Dipole Functionalized Triphenylene-Based Discotic Liquid Crystals Revealed by Broadband Dielectric Spectroscopy and Advanced Calorimetry – Assessment of The Molecular Origin. *Phys. Chem. Chem. Phys.* **2019**, *21* (33), 18265-18277.
[35] Yildirim, A.; Kolmangadi, M.; Bühlmeyer, A.; Huber, P.; Laschat, S.; Schönhals, A. Electrical Conductivity and Multiple Glassy Dynamics of Crown Ether-Based Columnar Liquid Crystals. *J. Phys. Chem. B* **2020**, *124* (39), 8728-8739.

Table of Contents graphic


Disc
tumbling
No columnar
order
fast cooling (> 50 K/s)
freezes disc tumbling
slow cooling
Isotropic
liquid
$T_{Col/I}$
Columnar
glass
Columnar
liquid crystal
Enthalpy
Temperature